# Chemical Science

Accepted Manuscript


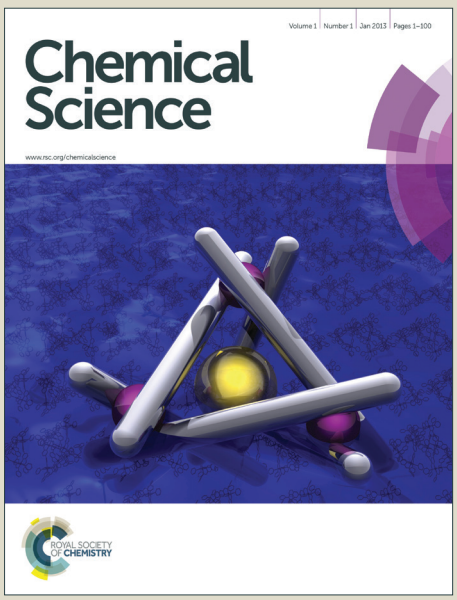





ROYAL SOCIETY OF CHEMISTRY

www.rsc.org/chemicalscience

# Light-Activated Antimicrobial Surfaces With Enhanced Efficacy Induced by a Dark-Activated Mechanism†

**Sacha Noimark,[a] Elaine Allan,[b] and Ivan P. Parkin*[a]**

***Received Xth XXXXXXXXXX 20XX, Accepted Xth XXXXXXXXX 20XX***
***First published on the web Xth XXXXXXXXXX 200X***
**DOI: 10.1039/b000000x**

Novel bactericidal surfaces were prepared by incorporating crystal violet, methylene blue and 2 nm gold nanoparticles into medical grade silicone using a simple dipping technique. The modified polymers were stable to cleaning by use of an alcohol-based wipe and demonstrated good photostability under intense illumination conditions. The photobactericidal activity of this polymer was compared against a range of other photobactericidal polymers against both *Staphylococcus epidermidis* and *Escherichia coli*, under white lighting conditions comparable to that found in a clinical environment. Not only did this novel multi-dye-nanogold-polymer exhibit the strongest photobactericidal activity reported to date, surprisingly, it also demonstrated significant antimicrobial activity under dark conditions.

## 1 Introduction

Hospital-acquired infections cost NHS hospitals over £1 billion each year in the UK[1]. Infections caused by staphylococci such as methicillin-resistant *Staphylococcus aureus*, *Clostridium difficile* and *Escherichia coli* have attracted media attention and hospitals are under extreme pressure to reduce and control the incidence of these infections. In fact, over the course of 2010 - 2011, the U.K. Government's Advisory Committee on "Antimicrobial Resistance and Healthcare-Associated Infection" recommended the extension of mandatory surveillance schemes to include two new national mandatory reporting schemes for bacteraemia due to *E. coli* and methicillin-susceptible *S. aureus*, in addition to the previously in place schemes for methicillin-resistant *S. aureus* (MRSA) and *C. difficile*.[2]

It has been estimated that in the United States, in the hospital Intensive Care Units, the endogenous microbiota of patients is a key source of pathogens, associated with approximately 40 - 60 % of nosocomial infection.[3,4] It is likely that hands of healthcare workers become contaminated from direct patient contact, or from exposure to colonised hospital surfaces. These surfaces act as reservoirs of bacteria and constant contact by healthcare personnel between these surfaces and patients aid the transfer of bacteria and facilitate the spread of infection within healthcare institutions.[5–7] Although rigorous cleaning regimes are enforced, it is difficult to prevent the contamination of touch surfaces in hospitals and despite promotion of healthcare worker hygiene protocols, in heavily contaminated areas, hand washing may be ineffectual.[7] Studies have demonstrated bacterial colonisation of a variety of hospital surfaces including: X-ray cassettes, door handles, mops, telephones, computers and keyboards, taps, pens, stethoscopes, sterile packaging and so forth.[7–15] Bacterial contamination on hospital touch surfaces is extremely prevalent, but these widespread infections are potentially avoidable. One strategy to reduce hospital contamination is the use of self-sterilising surfaces (Figure 1). By utilising an antimicrobial surface, the transmission of bacteria from surfaces to patients and from surfaces to healthcare workers, is disrupted and potentially, may effect a decrease in the spread of infection in healthcare environments.

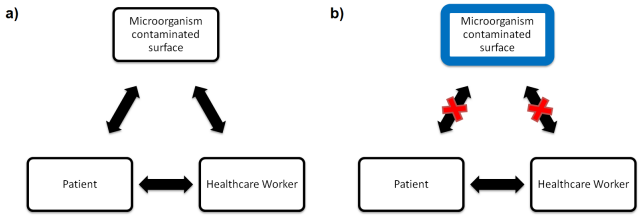


**Fig. 1** The role of surfaces in the transmission of hospital infection. a) Cycle of bacterial transfer from surfaces to patients. b) Disruption of cycle due to the use of an antimicrobial surface

Much research has focused on employing a range of syn-

† Electronic Supplementary Information (ESI) available: [details of any supplementary information available should be included here]. See DOI: 10.1039/b000000x/

[a] *Materials Chemistry Research Centre, Department of Chemistry, University College London, 20 Gordon St, London, WC1H 0AJ, UK; Tel: +44 207 679 4669; E-mail: i.p.parkin@ucl.ac.uk*
[b] *Division of Microbial Diseases, UCL Eastman Dental Institute, University College London, 256 Grays Inn Road, London, WC1X 8LD, UK*

thetic strategies to develop both hard and soft antimicrobial surfaces[5,7,16]. Examples include: deposition of $TiO_2$, doped-$TiO_2$ films onto hard surfaces,[17–22] silver ion technology,[23,24] copper coated or incorporated surfaces,[25–28] the covalent attachment of quaternary ammonium salts to polymeric surfaces,[29,30] microbicide-releasing surfaces,[31,32] in addition to the incorporation of photosensitiser dyes into polymers.[33–45] The latter, termed antimicrobial photodynamic therapy, is a particularly interesting approach since photosensitisers can inactivate micro-organisms via multiple, conserved targets giving a broad spectrum of activity and low risk of resistance development.

An alternative approach that circumvents the synthetic difficulties of strategic covalent attachment of antimicrobial molecules to polymeric materials, is the utilisation of a 'swell-encapsulation-shrink' technique. This simple yet effective strategy to incorporate photosensitiser dyes into medical grade polymers results in the development of efficacious light-activated antimicrobial materials that induce the lethal photosensitisation of both Gram-positive and Gram-negative bacteria upon either short-term illumination using a laser light source (order of minutes), or over a slightly longer-term irradiation duration, using a standard hospital light source to activate the antimicrobial properties of the surfaces (order of hours).[33–36,38,40–45] In these investigations, it has also been found that in the case of certain photosensitisers, the additional encapsulation of 2 nm gold nanoparticles significantly enhances the photo-activity of the dye.[35,36,38,40,41] Time-resolved EPR studies indicated that the enhancement in the demonstrated photo-activity of the dye incorporated polymer can be attributed to an increased dye triplet state production when 2 nm gold nanoparticles are present.[38] Recent research has primarily been targeted towards the development of potent light-activated antimicrobial materials for use in medical devices, that require laser-irradiation to activate the bactericidal properties.[33–38,40] However, some research on the incorporation of photosensitiser dyes into polymers for use as a material for touch surfaces in a clinical environment has been achieved.[41–45]

In this paper we report on the efficacious bactericidal activity of medical grade silicone encapsulated with methylene blue and 2 nm gold nanoparticles, coated with crystal violet dye; a multi-dye-nanogold combination. The modified polymers were prepared by use of a novel two-step dipping process and the materials were characterised using UV-Vis absorbance spectroscopy. Functional testing of the material included an examination of the wetting properties, in addition to an extensive photostability investigation. Microbiological testing of the new material involved a comparison with previously synthesised photosensitiser-incorporated silicones against both a Gram-positive and a Gram-negative bacterium, using a white light source comparable to standard hospital lighting conditions to activate the antimicrobial properties of the polymers. The multi-dye-nanogold incorporated polymer demonstrated the most potent photobactericidal activity upon white light illumination ever reported and surprisingly for the first time, significant dark kill of both *S. epidermidis* and *E. coli* was observed. This later fact is a significant step-forward for dye-based antimicrobial surfaces, as it indicates that they can be efficacious under any lighting conditions.

## 2 Experimental

### 2.1 Materials Synthesis

A series of samples were prepared for microbiological testing using a novel two-step dipping method. NuSil silicone polymer squares were immersed in a swelling solution for 72 h as described in Table 1. After air-drying (24 h), the samples were washed and towel-dried, after which selected samples (see table) were subsequently immersed in a crystal violet dipping solution (72 h). The samples were then air-dried again, washed and towel-dried (Figure 2).

**Table 1** Dipping conditions for material preparation. Where possible the samples were maintained under dark conditions

| Dipping Solution | Control | MBAu | CV | CVAu | CVMBAu |
|---|---|---|---|---|---|
| 9:1 acetone:water | y | - | - | - | - |
| 9:1 acetone:nanogold | | y* | - | y | y* |
| 0.001 M CV solution | - | - | y | y | y |

* dipping solution saturated with methylene blue (700 mg/mL)

### 2.2 Materials Characterisation

The UV-Vis absorption spectra of the treated silicone polymers prepared for microbiological testing were measured using a PerkinElmer Lambda 25 UV-Vis Spectrometer, within the range 400 - 750 nm. A Bruker Platinum ATR was used

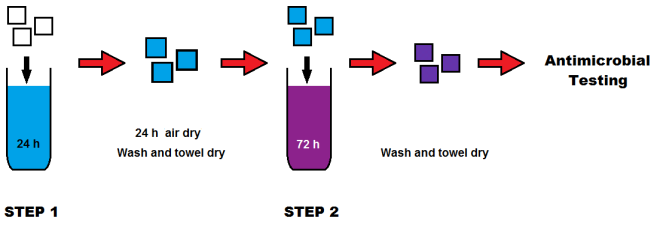


**Fig. 2** Schematic to show preparation of CVMBAu sample

to measure the infrared absorbance spectra of the samples, within the range 4000 - 400 $cm^{-1}$ with an accumulation of 15 scans per sample.

### 2.3 Dye Adherence Testing

The crystal violet-coated and crystal violet-coated, methylene blue and nanogold-encapsulated silicone samples were wiped rigorously with a 70% isopropyl alcohol wipe (AZOwipe™, Synergy Health) to determine whether the dye adhered to the sample surface under standard cleaning regimes.

### 2.4 Sample Photostability Testing

Treated polymer samples were stored in a white light box for an extended duration. The samples were exposed to intense white lighting conditions using a white light source (General Electric 28 W Watt Miser™ T5 2D compact fluorescent lamp) emitting an average light intensity of 12,500 $\pm$ 250 lux at a distance of 16 cm from the samples.

### 2.5 Wetting Properties

Equilibrium water contact angle measurements ($\sim$8.75 $\mu$L) on: untreated silicone, solvent treated (control) silicone, crystal violet-coated silicone, methylene blue and 2 nm gold nanoparticle-encapsulated silicone and crystal violet-coated nanogold encapsulated silicone, were also obtained. The contact angle measurement for each sample type was taken to be the average value over $\geq$10 measurements, using a droplet of deionised water dispensed by gravity from a gauge 27 needle and the samples were photographed side on. The data was analysed using FTA32 software.

### 2.6 Antimicrobial Activity

A range of silicone elastomer samples (1.1 cm x 1.1 cm) were used in the microbiology experiments: solvent treated (control), crystal violet-coated, methylene blue and 2 nm gold nanoparticle-encapsulated, crystal violet-coated nanogold-encapsulated and crystal violet-coated, methylene blue and nanogold-encapsulated medical grade silicone. These samples were tested against *S. epidermidis* RP62a and *E. coli* NCTC 25522. These organisms were stored at -70 °C in Brain-Heart-Infusion broth (BHI, Oxoid) containing 20 % (v/v) glycerol and propagated on either Mannitol Salt agar (MSA, Oxoid) in the case of *S. epidermidis*, or MacConkey agar (MAC, Oxoid Ltd.) in the case of *E. coli*, for a maximum of two sub-cultures at intervals of two weeks.

BHI broth (10 mL) was inoculated with 1 bacterial colony and cultured in air at 37 °C for 18 h with shaking, at 200 rpm. The bacterial pellet was recovered by centrifugation (21 °C, 1771 x*g*, 5 min), washed in phosphate buffered saline (PBS) and centrifuged again to recover the bacteria, which were finally re-suspended in PBS (10 mL). The washed suspension was diluted 1000-fold to obtain the inoculum ($\sim 10^6$ cfu /mL). The inoculum in each experiment was confirmed by plating ten-fold serial dilutions on agar for viable counts. Triplicates of each polymer sample type were inoculated with 25 $\mu$L of the inoculum and covered with a sterile cover slip (22 mm x 22 mm). The samples were then irradiated for up to $\sim$ 6 hours using a white light source (General Electric 28 W Watt Miser™ T5 2D compact fluorescent lamp) emitting an average light intensity of 3750 $\pm$ 250 lux at a distance of 30 cm from the samples. A further set of samples (in triplicate) was maintained in the dark for the duration of the irradiation time, whilst an additional sample set was maintained under dark conditions for up 18 hours.

Post irradiation, the inoculated samples and cover slips were added to PBS (225 $\mu$L) and vortexed. The neat suspension and ten-fold serial dilutions were plated on the appropriate agar for viable counts. The plates were incubated aerobically at 37 °C for 24 h (*E. coli*) or 48 h (*S. epidermidis*). Each experiment contained 3 technical replicates and the experiment was reproduced three times. The Mann-Whitney U test was used to determine the significance of the following comparisons: (i) the activity of each of the modified polymers compared to the control silicone sample when both were incubated in the dark and (ii) the activity of each the irradiated modified polymers compared to the same material incubated in the dark.

## 3 Results and discussion

### 3.1 Materials Synthesis and Characterisation

The use of a 'one-step' or 'two-step' dipping strategy to incorporate photosensitiser dyes in addition to 2 nm gold nanoparticles into medical grade polymers, has been detailed in the literature.[34–36,38,40,42] In this work we used a novel 'two-step' method to develop a polymer encapsulated with a dual photosensitiser dye combination, in addition to 2 nm gold nanoparticles. In the first step, the silicone samples were immersed in a 9 : 1 acetone : nanogold swelling solution saturated with methylene blue dye. Upon exposure to the solvent, the polymer swells enabling the dye molecules to diffuse through the polymer. When the silicone is removed

from the swelling solution, the residual solvent evaporates resulting in a dye-incorporated polymer. In the subsequent step, the treated polymer sections were immersed in a 1 x $10^{-3}$ mol $dm^{-3}$ crystal violet solution for 72 hours such that the resultant polymer is coated with a thin layer of crystal violet dye at the polymer surface. Although the mechanistic details are unclear, it is clear that the crystal violet dye strongly attaches to the polymer surface under aqueous dipping conditions, as the polymer sections showed no detectable leaching of crystal violet. Samples incorporated with methylene blue in addition to crystal violet were a blue-purple colour, whereas those exposed to just the crystal violet were a more purple hue (Figure 3b). It should be noted that the presence of 2 nm gold nanoparticles did not affect the sample colouration.

The dye-incorporated samples were analysed using UV-Vis spectroscopy within the range 400 - 800 nm and their absorbance spectra were compared to that of a hospital lighting emission spectrum (Figure 3a). From the spectra it is clear that the crystal violet-coated, nanogold-encapsulated silicone sample absorbed strongly at 594 nm with a shoulder peak at 548 nm, whereas the methylene blue immobilised in the silicone sample demonstrated a maximum absorption at 651 nm with small shoulder peaks at ~610 nm and ~670 nm. The UV-Vis absorbance signal of the crystal violet-coated, methylene blue and nanogold encapsulated sample exhibited

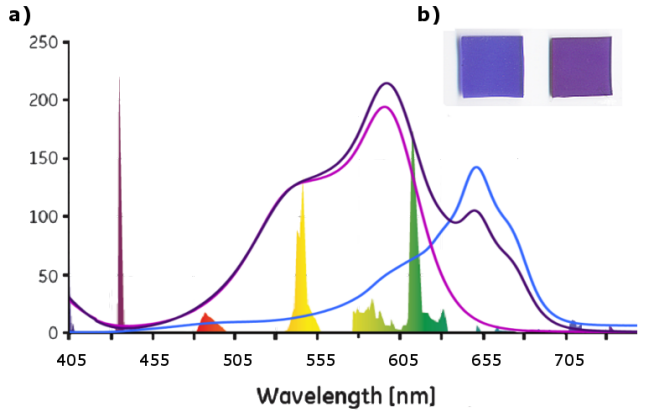


**Fig. 3** a) Hospital lighting emission spectrum of a 28-W fluorescent lamp[46] with UV-Vis spectra of a series of treated silicone polymers overlayed. The UV-vis absorbance spectra of methylene blue and nanogold encapsulated silicone (blue line), crystal violet-coated, nanogold-encapsulated silicone (violet line) and crystal violet coated, methylene blue and nanogold encapsulated silicone (purple line) were measured within the range 380 - 750 nm. The absorbance spectra were scaled and therefore no y-axis units are provided. b) Crystal violet-coated nanogold and methylene blue-encapsulated silicone and nanogold encapsulated silicone samples, prepared using a novel 2-step dipping protocol

key peaks from both the individual samples, with peak maxima in the same wavelength region at 594 nm and 651 nm and shoulder peaks at 548 nm and 670 nm, corresponding to the crystal violet and methylene blue respectively. The presence of the 2 nm gold nanoparticles affected neither the dye peak intensity, shape, nor position compared to samples incorporated with dye only and the UV-Vis spectra of the dye/nanogold-incorporated samples demonstrated no detectable absorbance in the visible region of the spectrum of the gold nanoparticles, as the small diameter of the nanoparticles used, is below the limit for surface plasmon resonance (4 nm).[36,40] It is also interesting to note that there appears to be little electronic interaction between the 2 dyes incorporated into the polymer, since the absorbance spectrum of the multi-dye silicone is effectively a 'sum' of the spectra of the individual dye incorporated silicones.

The infrared absorbance spectra of the silicone samples prepared for the microbiological testing, in addition to an untreated silicone sample, were obtained by ATR. No significant difference in the measured spectra was evident, across the sample range analysed (supplementary data). This can be attributed to the strong absorbance bands of the silicone substrate, which presumably masks any weak signals from the dye. The absorbance patterns obtained were expected, due to the relatively low dye concentrations present in the polymers. However, the similarity in the spectra (characteristic of that of the untreated silicone sample), indicated that the solvent treatment did not detrimentally affect the polymer substrate, in terms of effecting a chemical change in the silicone polymer.

**Table 2** Average water contact angle measurements (°) ± standard deviation, of water on a range of silicone polymers: untreated, solvent treated (control), methylene blue and 2 nm gold nanoparticle encapsulated (MBAu), crystal violet-coated (CV), crystal violet-coated, 2 nm gold nanoparticle encapsulated (CVAu) and crystal violet-coated, methylene blue and 2 nm gold nanoparticle encapsulated (CVMBAu)

| Silicone Sample | Contact Angle (°) | ± | Standard Deviation |
|---|---|---|---|
| Untreated | 102 | ± | 1.0 |
| Control | 101 | ± | 1.5 |
| MBAu | 100 | ± | 0.3 |
| CV | 100 | ± | 0.5 |
| CVAu | 100 | ± | 0.5 |
| CVMBAu | 102 | ± | 0.8 |

### 3.2 Functional Properties

The modified polymers were wiped rigorously with 70 % alcohol and there was no visual evidence of dye removal from the treated polymer surface under these cleaning conditions, indicating the modified polymers should be stable with respect to standard hospital cleaning protocol. This test is extremely important, since despite the potent antimicrobial nature of these polymers, it is anticipated that surfaces treated by this method may still undergo the regimented hospital cleaning protocol and thus, must be stable to robust wiping using an alcohol-based, anti-infective wipe.

The wetting properties of a range of untreated and treated silicone samples were measured under laboratory temperature and lighting conditions. From the water contact angle measurement data (Table 2), it can be inferred that the untreated silicone presents a hydrophobic surface and the treatment of the polymers to incorporate dyes, dye-nanogold combinations or dye-dye-nanogold combinations effects negligible differences in the subsequent wetting properties of the surfaces.

UV-Vis spectroscopy was employed to investigate the photostability of the dye incorporated silicone polymers upon exposure to a white light source - 8W GE lighting (3500 K) - commonly used in UK hospitals (for emission spectrum, see Figure 3a). The measured light intensity at the samples was $\sim$ 12, 500 lx at a distance of 16 cm from the light source. The absorbance of the illuminated samples was measured periodically within the range 400 - 800 nm (Figure 4).

The lighting conditions used in this study can be considered in relation to the brightness of various areas in UK healthcare environments, as recommended by the Department of Health (Table 3)[17] and it was found that they were $\sim$ 125 x more intense than those typically found in hospital corridors and wards; areas in which microbial contamination is prevalent. Under these intense irradiation conditions, the photodegradation of the crystal violet was $\sim$ 51 % for the crystal violet-coated, nanogold-encapsulated silicone sample and $\sim$ 81 % for the crystal violet-coated, methylene blue and nanogold-encapsulated silicone sample, over the course of up

**Table 3** Recommended light intensities for different areas in UK healthcare environments [17,44]

| Environment | Light Intensity /lx |
|---|---|
| Operating theatre | 10,000 - 100,000 |
| A & E Examination Room | 1,000 |
| Ward corridors | $\geq$ 200 |
| Typical dental chair* | 250 |

* Measurement performed at UCLH Eastman Dental Hospital

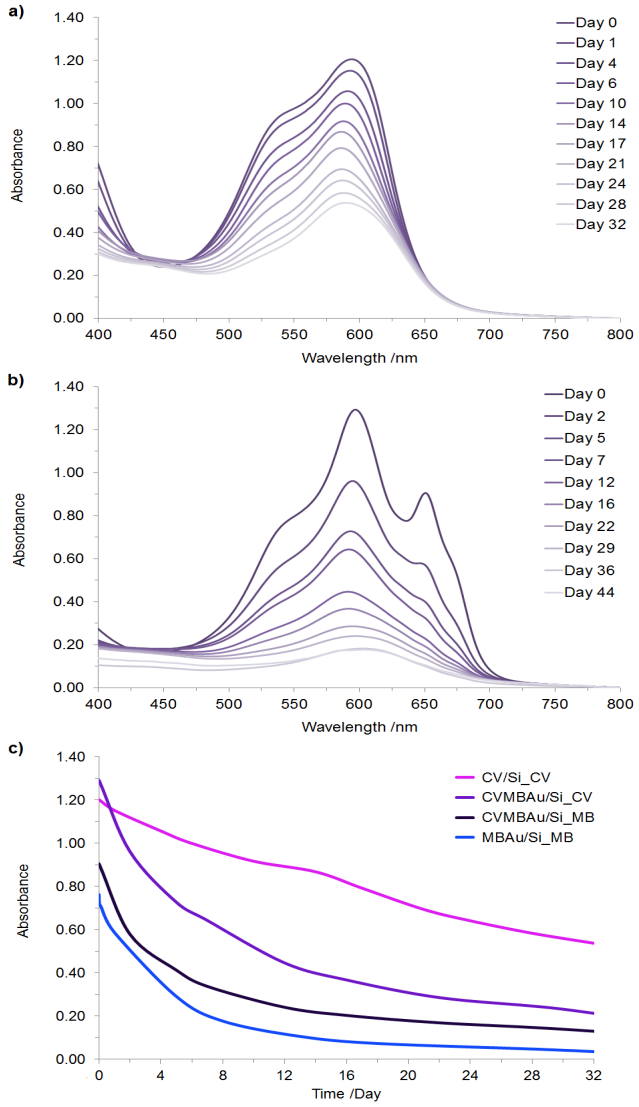


**Fig. 4** UV-Vis absorbance spectra measured in the range 400 - 800 nm of a) crystal violet-coated nanogold encapsulated silicone and b) crystal violet-coated, methylene blue and nanogold-encapsulated silicone using a simple dipping method. The samples were illuminated with a white light source emitting an average light intensity of 12,500 $\pm$ 250 lux at a distance of 16 cm from the samples. c) Rate of photodegradation of modified polymers upon exposure to white light illumination (32 days, 12,500 lx). The rate is displayed as a decrease in sample absorbance at the absorbance maxima, over time. CV/Si_CV represents the crystal violet peak in the crystal violet-coated, nanogold encapsulated silicone sample, CVMBAu/Si_CV and CVMBAu/Si_MB represents the crystal violet and methylene blue peaks in the crystal violet-coated, methylene blue and nanogold-encapsulated silicone sample respectively and MBAu/Si_MB represents the methylene blue peak in the methylene blue and nanogold-encapsulated polymer

to 29 days (Figure 4c). It is anticipated that the degradation of these dyes correlates to the light-flux levels and thus, the samples tested indicate strong stability and suitability for these antimicrobial surfaces to be employed in a clinical environment such as hospital wards, where they would be expected to maintain potency for ca. 10 years (based on light-flux levels used).

### 3.3 Bactericidal Properties

We report the antimicrobial activity of multi-dye-nanogold-encapsulated silicone sample systems and compare it to a series of other dye and dye-nanogold embedded silicones developed previously. The samples were tested against a Gram-positive bacterium and a Gram-negative bacterium, *S. epidermidis* and *E. coli*, respectively. The data show that the antimicrobial activity of the polymers was promoted by exposure of the samples to a white hospital light source; a compact fluorescent lamp which emits light across the visible region of the spectrum and is similar to those commonly found in U.K. hospitals. In all experiments, a control sample set was maintained under dark conditions for the same period of time as the samples exposed to light and in a further experiment, a sample set was incubated under dark conditions for an extended time period. The antimicrobial activity of crystal violet-coated silicone (CV), crystal violet-coated, nanogold-encapsulated silicone (CVAu), methylene blue and nanogold encapsulated silicone (MBAu) and crystal violet-coated, methylene blue and nanogold-encapsulated silicone (CVMBAu) was compared to that of a control, solvent treated silicone sample.

The lethal photosensitisation induced by these samples when exposed to a white light source emitting an average light intensity of $3750 \pm 250$ lux at a distance of 30 cm from the samples, is demonstrated in Figure 5((a)-(c)). In dark conditions for incubation times of 3 h, the methylene blue and nanogold-encapsulated sample exhibited no statistically significant kill of *S. epidermidis* when compared to the control silicone sample. However, all crystal violet-coated silicone samples demonstrated statistically significant ($P < 0.001$) bacterial kills compared to the control silicone sample, ranging from a 0.76 log reduction in bacterial numbers with CV alone to a 1.9 log kill with CVMBAu, within 3 hours of contact time in the dark (Figure 5(a)). Upon illumination with white light (3 h), all dye-incorporated samples demonstrated strong light-activated antimicrobial activity, with statistically significant kills compared to the same dye-incorporated samples stored in dark conditions for an equivalent time period ($P < 0.001$). The crystal violet-coated silicone sample types encapsulated with 2 nm gold nanoparticles exhibited the most efficacious light-activated activity against *S. epidermidis*, with bacterial numbers reduced below the detection limit in 3 h.

Novel photo-activated antimicrobial surfaces that also show significant antimicrobial activity against a Gram-negative bacterium under dark conditions, have been developed. When tested against *E. coli*, all crystal violet-coated silicone samples demonstrated statistically significant bactericidal activity against *E. coli* upon incubation under dark conditions for 3 hours (Figure 5(b); $P < 0.01$ (CV) and $P < 0.001$ (CVAu, CVMBAu)), with increased antimicrobial activity exhibited when incubated for 6 hours and 18 hours (Figure 5(c) and Figure 5(d)). The efficacy of the bactericidal activity against *E. coli* demonstrated by these surfaces varied across the sample range and, as was the case when tested against *S. epidermidis*, the CVMBAu sample surface effected the greatest reduction in bacterial numbers of up to 1.49 log, when incubated for time periods of up to 18 hours in the dark. The CVAu sample also showed strong antimicrobial activity, resulting in up to 0.66 log kills against *E. coli* when in contact with the modified silicone surface for up to 18 hours. The MBAu sample demonstrated no statistically significant activity against *E. coli* despite an extended incubation in dark conditions, when compared to the control silicone sample.

The nanogold-attributed enhancement in the lethal photosensitisation of Gram-negative bacteria on photosensitiser-incorporated silicone under conditions of white light illumination, was also examined. All modified silicone samples exhibited photo-activated bactericidal activity against *E. coli*. Although statistically significant kills were achieved in all cases for the treated silicone samples when compared to the corresponding samples under dark conditions ($P < 0.001$), the extent to which the lethal photosensitisation of *E. coli* was achieved by these surfaces varied greatly across the sample range. The modified sample that demonstrated the least bactericidal activity compared to the silicone control upon activation with a white hospital light source, was the methylene blue and nanogold-encapsulated silicone, with limited kills achieved even after 6 hour illumination. The CV sample demonstrated stronger photo-activity than the MBAu samples, although the presence of 2 nm gold nanoparticles significantly enhanced the bacterial kills achieved on the crystal violet-coated silicone surfaces, by a factor of $> 1.15$ log.

The novel multi-dye-nanogold silicone samples developed not only demonstrated potent bactericidal activity under dark conditions, but these samples also induced the lethal photosensitisation of *E. coli*, with bacterial numbers reduced by $> 2.1$ log upon 3 hours exposure to white light and reduction to below the detection limit within 6 hours of white

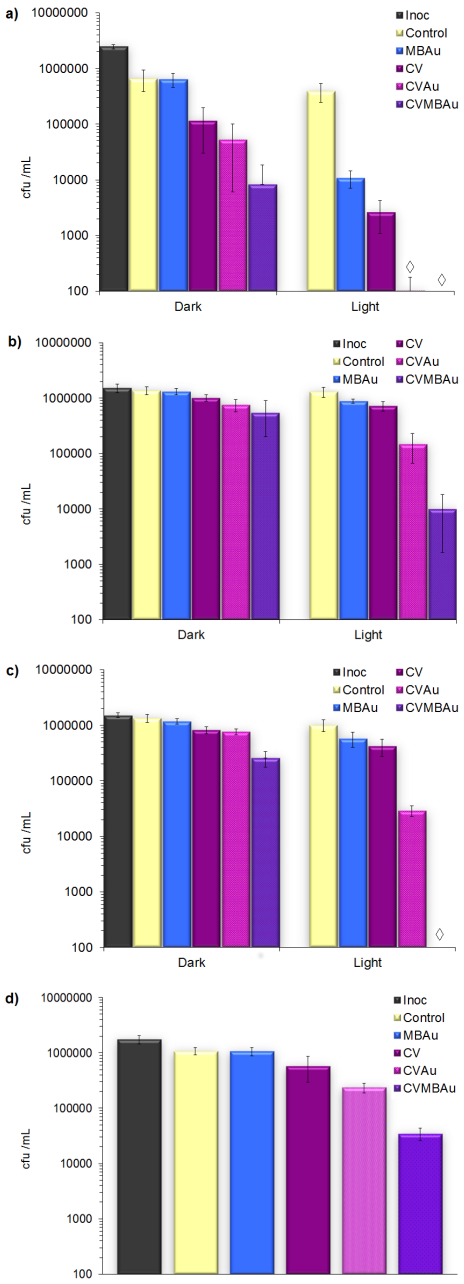


**Fig. 5** Viable counts of bacteria after incubation on modified silicone polymers exposed to white light illumination: (a) *S. epidermidis* (3 h illumination), (b) *E. coli* (3 h illumination) and (c) *E. coli* (6 h illumination). The white light source emitted an average light intensity of 3,500 ± 250 lux at a distance of 30 cm from the samples. (d) Viable counts of *E. coli* from the surface of samples incubated at 20°C for 18 h under dark conditions. ◇ Indicates that the bacterial numbers were reduced to below the detection limit of 100 cfu

light illumination. These multi-dye samples utilise a greater proportion of light emitted from the white light source, with sample absorbance within the region 475 - 700 nm (see Figure 3). Consequently, there is greater potential for the generation of reactive oxygen species - the cytotoxic species that initiate multi-site attack against bacteria - since dye excitation can occur over a greater range of wavelengths due to the multiple dyes incorporated in the silicone.

Contrary to previously synthesised materials, we have developed and reported here potent photobactericidal polymers that *also* demonstrate significant dark kill, predominantly against the Gram-positive bacterium, *S. epidermidis*, but also against the Gram-negative bacterium, *E. coli*. This has been achieved by incorporating the triarylmethane photosensitiser dye, crystal violet, into the nanogold or methylene blue and nanogold encapsulated silicone, by use of a novel two-step dipping strategy. Although the anti-infective properties of crystal violet were first discovered in the 1890s by Stilling, it was Churchman (1912) who noted the selective action of the dye against Gram-positive bacteria.[47–50] Crystal violet has since been used as a treatment for infected wounds and superficial skin infections, with clinical trials regarding its use as a potential treatment against MRSA[51,52] and was an important topical antiseptic, before modern drugs replaced it.[50] The use of gentian violet as a treatment for skin conditions such as superficial wounds, fungal infections and infected scabies was recommended by the World Health Organisation for inclusion in 'The Interagency Emergency Health Kit'.[2] The photo-activated antimicrobial effect of crystal violet solution on *Porphyromonas gingivalis* has also been investigated using a rat model with a subcutaneous abscess, to determine the antimicrobial efficacy of this system in vivo, for potential clinical use to reduce bacterial plaque formation.[52]

Results indicate that crystal violet coating the silicone samples we have prepared, significantly increases the susceptibility of the Gram-positive bacterium, *S. epidermidis*, within 3 hours. A statistically significant, but more limited increase in sensitivity was demonstrated by *E. coli*, although this effect required far longer incubation times (18 hours). Interestingly, the results suggest that the encapsulation of gold nanoparticles into the silicone sample enhances not only the light-activated antimicrobial properties, but the inherent antimicrobial properties of the crystal violet dye itself. It can be speculated that there may be an interaction between the dye molecules and the gold nanoparticles that enhance its antimicrobial action. A similar effect has recently been noted in the literature, with regard to antibiotics and gold nanoparticles, in which the binding of antibiotics to spherical gold nanoparticles effects an enhancement in antimicrobial activity.[53–55] The results of this study show that this potential

crystal violet-nanoparticle interaction also increases the sensitivity of the Gram-negative bacterium, *E. coli*, towards the dye (Figure 5(d)). Following this reasoning, it can be further speculated that dye-dye interactions transpire, perhaps on the surface of the gold nanoparticles, since silicone samples embedded with methylene blue and gold nanoparticles in addition to crystal violet, consistently demonstrate greater efficacy in terms of their antimicrobial activity, compared to the sum kill of samples incorporated with only methylene blue and gold nanoparticles or crystal violet and gold nanoparticles.

The microbiological testing studies indicate that the crystal-violet incorporated samples outperform the methylene blue and nanogold-encapsulated samples under both dark conditions and white light illumination. It can be speculated that the increased efficacy in the photo-activated kill is due to the high concentration of crystal violet accumulated on the crystal violet sample surfaces.[40] It has previously been estimated that the reactive oxygen species, singlet oxygen, has a very short diffusion distance of around 0.2 microns within the polymer.[40] Consequently, in the case of the MBAu sample, since the dye is distributed relatively evenly throughout the polymer, the dye encapsulated within the polymer bulk is redundant with respect to contribution to the exhibited antimicrobial activity. Only dye embedded near the polymer surface will act in the photosensitisation of bacteria, as only the reactive oxygen species generated near to the polymer surface, rather than that generated within the bulk, will act to photo-damage bacteria. With high concentrations of photosensitiser on the crystal violet-coated polymer surfaces, there is a greater probability of the generation of cytotoxic reactive oxygen species within range of 'attack' against bacteria colonising the surface, subsequently contributing to the increased bacterial kills. It should also be noted, that the silicone surface accumulation of crystal violet dye may also contribute to the dark kill exhibited by the crystal violet-coated samples, since the bacteria are in direct contact with high surface concentrations of the antimicrobial agent.

It is anticipated that these bactericidal surfaces can be employed in hospitals for use in touch surfaces, including but not limited to: tablet and mobile phone covers and screen protectors, computer keyboards, hand-dryers and paint films, to help maintain low bacterial levels and hence, potentially reduce the risk of the spread of infection. In addition, it is envisaged that this technology can also be applied for use in medical devices such as catheters and endotracheal tubing, however, a low power laser irradiation system will be required for these applications. These novel samples demonstrate efficacious antimicrobial activity when tested against both Gram-positive and Gram-negative bacteria, commonly associated with nosocomial infection. Moreover, illumination with a white light source similar to that typically found in a hospital setting resulted in a strong enhancement in the antimicrobial activity demonstrated. The intensity of the white light source used to activate the photobactericidal properties of these polymers was $\sim$ 10 x that typically found in hospital ward corridors and $\sim$ 2 x that found in Accident and Emergency examination rooms (see Table 3).[17,44] Consequently, the photobactericidal activity of these surfaces would be most efficacious in examination rooms where the light intensity is higher, however, it is anticipated that significant kills can still be achieved in areas of lower light intensity if the irradiation time is prolonged. Moreover, in these experiments, very high bacterial loads ($\sim$ 32,920 cfu /cm$^2$ *E. coli*, $\sim$ 51,147 cfu /cm$^2$ *S. epidermidis*) were used to test the potency of these antimicrobial polymers, whereas on hospital surfaces, the bacterial on contaminated surfaces are considerably lower (up to an equivalent of 3060 cfu /cm$^2$ with average values of $<$ 100 cfu /cm$^2$).[56–59]

## 4 Conclusions

For the first time, we have developed potent light-activated antimicrobial surfaces that also demonstrate effective dark kill using polymers incorporated with multi-dye-nanogold combinations. Using a standard hospital white light source to activate the photobactericidal properties, these efficacious antimicrobial surfaces induced the lethal photosensitisation of *S. epidermidis* in just 3 hours and of *E. coli* in just 6 hours, with bacterial numbers reduced below the detection limit. The multi-mechanism antimicrobial activity proves attractive in terms of potential applications for use in a variety of hospital surfaces, as low bacterial levels will be maintained under non-optimal lighting conditions (i.e. at night, or when lights are dimmed), with a boost in antimicrobial activity achieved with increasing illumination intensity. Further work will include an examination of the efficacy of the bactericidal activity of these surfaces in a clinical environment.

## 5 Acknowledgements

IPP and SN thank the EPSRC and Ondine Biopharma for their financial support. The authors also thank Dr A J MacRobert and Dr K Page for helpful discussions

## References

1 *National Audit Office: Reducing Healthcare Associated Infections in Hospitals in England*, 12 June 2009.
2 *World Health Organization; The interagency emergency health kit*, 2006.

3 D. J. Weber, D. Anderson and W. A. Rutala, *Current opinion in infectious diseases*, 2013, **26**, 338–44.
4 R. A. Weinstein, *The American Journal of Medicine*, 1991, **91**, S179–S184.
5 S. Noimark, C. W. Dunnill and I. P. Parkin, *Advanced Drug Delivery Reviews*, 2013, **65**, 570–580.
6 B. Hota, *Clinical Infectious Diseases*, 2004, **39**, 1182–1189.
7 K. Page, M. Wilson and I. P. Parkin, *Journal of Materials Chemistry*, 2009, **19**, 3819–3831.
8 J.-S. Kim, H.-S. Kim, J.-Y. Park, H.-S. Koo, C.-S. Choi, W. Song, H. C. Cho and K. M. Lee, *Annals of Laboratory Medicine*, 2012, **32**, 206–209.
9 S. Oie, I. Hosokawa and A. Kamiya, *Journal of Hospital Infection*, 2002, **51**, 140–143.
10 S. Oie and A. Kamiya, *Journal of Hospital Infection*, 1996, **34**, 145–149.
11 P. Ciragil, M. Gul and M. Aral, *Journal of Hospital Infection*, 2006, **62**, 247–248.
12 S. Bures, J. T. Fishbain, C. F. T. Uyehara, J. M. Parker and B. W. Berg, *American Journal of Infection Control*, 2000, **28**, 465–471.
13 D. Banerjee, A. Fraise and K. Chana, *Journal of Hospital Infection*, 1999, **43**, 73–75.
14 H. A. Cohen, J. Amir, A. Matalon, R. Mayan, S. Beni and A. Barzilai, *Family Practice*, 1997, **14**, 446–449.
15 B. Dietze, A. Rath, C. Wendt and H. Martiny, *Journal of Hospital Infection*, 2001, **49**, 255–261.
16 S. Noimark, C. W. Dunnill, M. Wilson and I. P. Parkin, *Chemical Society Reviews*, 2009, **38**, 3435–3448.
17 C. W. Dunnill, K. Page, Z. A. Aiken, S. Noimark, G. Hyett, A. Kafizas, J. Pratten, M. Wilson and I. P. Parkin, *Journal of Photochemistry and Photobiology a-Chemistry*, 2011, **220**, 113–123.
18 Z. A. Aiken, G. Hyett, C. W. Dunnill, M. Wilson, J. Pratten and I. P. Parkin, *Chemical Vapor Deposition*, 2010, **16**, 19–22.
19 C. W. Dunnill and I. P. Parkin, *Dalton Transactions*, 2011, **40**, 1635–1640.
20 C. W. Dunnill, Z. Ansari, A. Kafizas, S. Perni, D. J. Morgan, M. Wilson and I. P. Parkin, *Journal of Materials Chemistry*, 2011, **21**, 11854–11861.
21 C. W. Dunnill, Z. A. Aiken, J. Pratten, M. Wilson and I. P. Parkin, *Chemical Vapor Deposition*, 2010, **16**, 50–54.
22 K. Page, R. G. Palgrave, I. P. Parkin, M. Wilson, S. L. P. Savin and A. V. Chadwick, *Journal of Materials Chemistry*, 2007, **17**, 95–104.
23 *AcryMed Inc., SilvaGard™ Technology Summary.*, www.acrymed.com/pdf/SilvaGard%20Technical%20Summary.pdf, Accessed: 2013-07-22.
24 *AgION Technologies Inc., AgION™ Technology.*, http://www.agion-tech.com, Accessed: 2013-07-22.
25 C. D. Salgado, K. A. Sepkowitz, J. F. John, J. R. Cantey, H. H. Attaway, K. D. Freeman, P. A. Sharpe, H. T. Michels and M. G. Schmidt, *Infection Control and Hospital Epidemiology*, 2013, **34**, 479–486.
26 F. Marais, S. Mehtar and L. Chalkley, *Journal of Hospital Infection*, 2010, **74**, 80–82.
27 A. Mikolay, S. Huggett, L. Tikana, G. Grass, J. Braun and D. H. Nies, *Applied Microbiology and Biotechnology*, 2010, **87**, 1875–1879.
28 T. J. Karpanen, A. L. Casey, P. A. Lambert, B. D. Cookson, P. Nightingale, L. Miruszenko and T. S. J. Elliott, *Infection Control and Hospital Epidemiology*, 2012, **33**, 3–9.
29 P. J. McCubbin, E. Forbes, M. M. Gow and S. D. Gorham, *Journal of Applied Polymer Science*, 2006, **100**, 381–389.
30 P. J. McCubbin, E. Forbes, M. M. Gow and S. D. Gorham, *Journal of Applied Polymer Science*, 2006, **100**, 538–545.
31 C. E. Edmiston, F. C. Daoud and D. Leaper, *Surgery*, 2013, **154**, 89–100.
32 D. L. Williams, K. D. Sinclair, S. Jeyapalina and R. D. Bloebaum, *Journal of Biomedical Materials Research Part B: Applied Biomaterials*, 2013, **101B**, 1078–1089.
33 S. Perni, J. Pratten, M. Wilson, C. Piccirillo, I. P. Parkin and P. Prokopovich, *Journal of Biomaterials Applications*, 2011, **25**, 387–400.
34 S. Perni, P. Prokopovich, C. Piccirillo, J. Pratten, I. P. Parkin and M. Wilson, *Journal of Materials Chemistry*, 2009, **19**, 2715–2723.
35 S. Perni, C. Piccirillo, J. Pratten, P. Prokopovich, W. Chrzanowski, I. P. Parkin and M. Wilson, *Biomaterials*, 2009, **30**, 89–93.
36 S. Perni, C. Piccirillo, A. Kafizas, M. Uppal, J. Pratten, M. Wilson and I. P. Parkin, *Journal of Cluster Science*, 2010, **21**, 427–438.
37 S. Perni, P. Prokopovich, I. P. Parkin, M. Wilson and J. Pratten, *Journal of Materials Chemistry*, 2010, **20**, 8668–8673.
38 S. Noimark, C. W. Dunnill, C. W. M. Kay, S. Perni, P. Prokopovich, S. Ismail, M. Wilson and I. P. Parkin, *Journal of Materials Chemistry*, 2012, **22**, 15388–15396.
39 C. Piccirillo, S. Perni, J. Gil-Thomas, P. Prokopovich, M. Wilson, J. Pratten and I. P. Parkin, *Journal of Materials Chemistry*, 2009, **19**, 6167–6171.
40 S. Noimark, M. Bovis, A. J. MacRobert, A. Correia, E. Allan, M. Wilson and I. P. Parkin, *RSC Advances*, 2013, **3**, 18383–18394.
41 S. Ismail, S. Perni, J. Pratten, I. Parkin and M. Wilson, *Infection Control and Hospital Epidemiology*, 2011, **32**, 1130–1132.
42 A. J. T. Naik, S. Ismail, C. Kay, M. Wilson and I. P. Parkin, *Materials Chemistry and Physics*, 2011, **129**, 446–450.
43 V. Decraene, J. Pratten and M. Wilson, *Infection Control and Hospital Epidemiology*, 2008, **29**, 1181–1184.
44 V. Decraene, J. Pratten and M. Wilson, *Applied and Environmental Microbiology*, 2006, **72**, 4436–4439.
45 V. Decraene, J. Pratten and M. Wilson, *Current Microbiology*, 2008, **57**, 269–273.
46 *White Light Source, Spectral Power Distribution*, http://www.gelighting.com/LightingWeb/emea/images/2D_Watt_Miser_DataSheet_tcm181-10576.pdf, Accessed: 2013-07-22.
47 J. W. Churchman, *Journal of Experimental Medicine*, 1912, **16**, 221–U50.
48 J. Stilling, *The Lancet*, 1890, **136**, 965–966.
49 J. Stilling, *The Lancet*, 1891, **137**, 872–873.
50 *Chicago: American Medical Association*, 1939.
51 M. Saji, S. Taguchi, K. Uchiyama, E. Osono, N. Hayama and H. Ohkuni, *Journal of Hospital Infection*, 1995, **31**, 225–228.
52 K. Kawamoto, N. Senda, K. Shimada, K. Ito, Y. Hirano and S. Murai, *Lasers in Medical Science*, 2000, **15**, 257–262.
53 H. Gu, P. L. Ho, E. Tong, L. Wang and B. Xu, *Nano Letters*, 2003, **3**, 1261–1263.
54 M. F. Zawrah and S. I. Abd El-Moez, *Life Science Journal-Acta Zhengzhou University Overseas Edition*, 2011, **8**, 37–44.
55 A. N. Grace and K. Pandian, *Colloids and Surfaces a-Physicochemical and Engineering Aspects*, 2007, **297**, 63–70.
56 M. G. Schmidt, I. Attaway, Hubert H., S. E. Fairey, L. L. Steed, H. T. Michels and C. D. Salgado, *Infection Control and Hospital Epidemiology*, 2013, **34**, 530–533.
57 M. G. Schmidt, H. H. Attaway, P. A. Sharpe, J. John, Joseph, K. A. Sepkowitz, A. Morgan, S. E. Fairey, S. Singh, L. L. Steed, J. R. Cantey, K. D. Freeman, H. T. Michels and C. D. Salgado, *Journal of Clinical Microbiology*, 2012, **50**, 2217–2223.
58 F. Marais, S. Mehtar and L. Chalkley, *Journal of Hospital Infection*, 2010, **74**, 80–82.
59 G. Hedin, J. Rynback and B. Lore, *Journal of Hospital Infection*, 2010, **75**, 112–115.